

# **Deep Learning-Based Diagnosis of Disease Activity in Patients with Graves' Orbitopathy Using Orbital SPECT/CT**

Ni Yao<sup>1</sup>, Longxi Li<sup>1</sup>, Zhengyuan Gao<sup>2</sup>, Chen Zhao<sup>3</sup>, Yanting Li<sup>1</sup>, Chuang Han<sup>1</sup>, Jiaofen Nan<sup>1</sup>, Zelin Zhu<sup>1</sup>, Yi Xiao<sup>4</sup>, Fubao Zhu<sup>1</sup>, Min Zhao<sup>4,5\*</sup>, Weihua Zhou<sup>3,6</sup>

<sup>1</sup>School of Computer and Communication Engineering, Zhengzhou University of Light Industry, Zhengzhou, Henan, 450002, China.

<sup>2</sup>School of Biomedical Engineering, Health Science Center, Shenzhen University, Shenzhen, 518060, China

<sup>3</sup>Department of Applied Computing, Michigan Technological University, Houghton, MI, USA.

<sup>4</sup>Department of Nuclear Medicine, Xiangya Hospital, Central South University, Changsha, China.

<sup>5</sup>National Clinical Research Center of Geriatric Disorders, Xiangya Hospital, Central South University, Changsha, China

<sup>6</sup>Center for Biocomputing and Digital Health, Institute of Computing and Cybersystems, and Health Research Institute, Michigan Technological University, Houghton, MI, USA.

\*Corresponding Authors:

Min Zhao, M.D, Ph.D

Xiangya Hospital of Central South University

No.87, Xiangya Road, Changsha, Hunan Province, China, 410008

TEL: 086-0731-84327430, FAX: 086-0731-84327430

E-mail: [mzhao1981@csu.edu.cn](mailto:mzhao1981@csu.edu.cn)

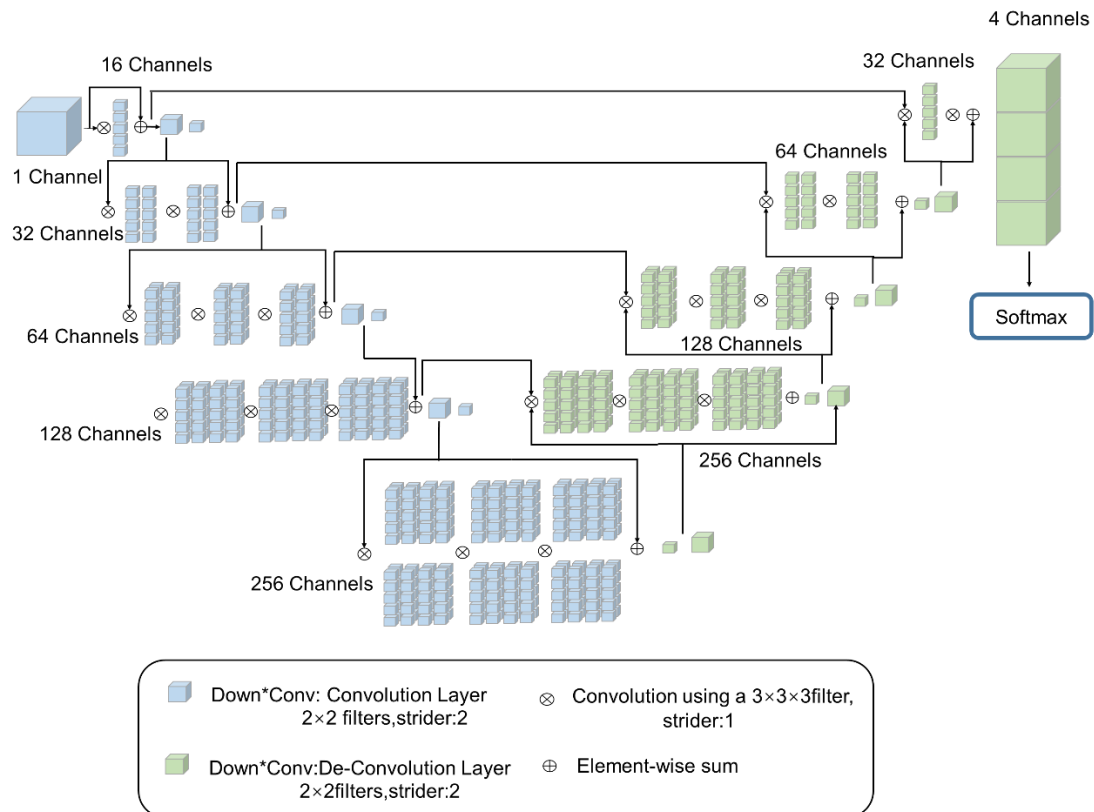
## Supplemental Table

**Supplemental Table 1 Performance of the classification model on the test set grouped by gender and age.**

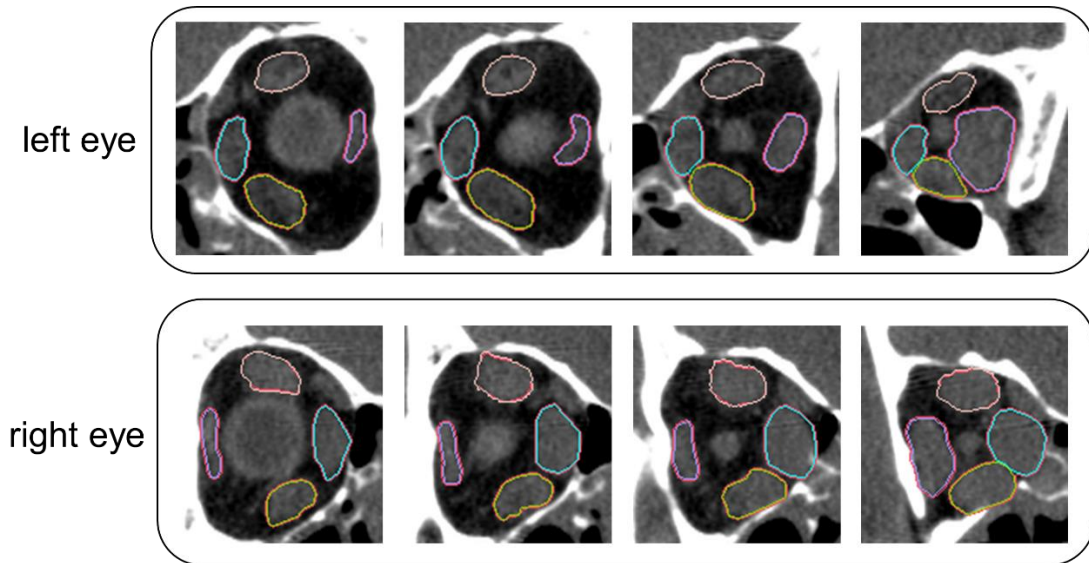
	Accuracy(%)	Precision(%)	Sensitivity(%)	Specificity(%)	F1-score
<b>Male</b>	89.67±1.46	87.32±1.81	92.61±1.07	86.81±2.08	0.89±0.01
<b>Female</b>	79.6±0.80	78.27±3.78	81.63±2.91	77.65±1.63	0.80±0.01
<b>Age &lt; 45</b>	83.03±1.34	78.55±2.29	76.84±2.00	86.89±1.80	0.78±0.02
<b>Age &gt;= 45</b>	84.89±1.24	87.97±1.51	87.02±1.79	81.62±2.65	0.87±0.01

## Supplemental Figure legends

**Supplemental Fig. 1 Flowchart of GO-Net architecture for segmentation.**

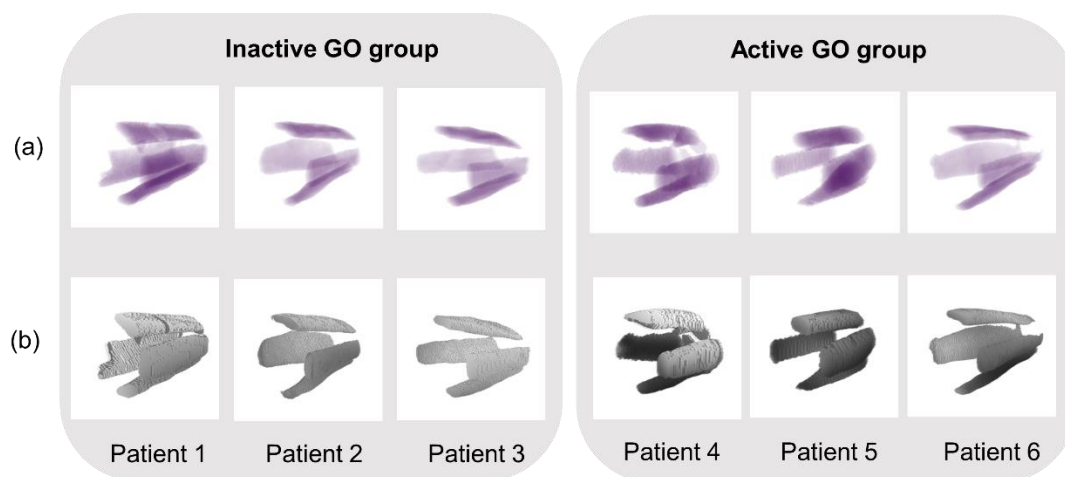


**Supplemental Fig. 2 Semantic segmentation results.**



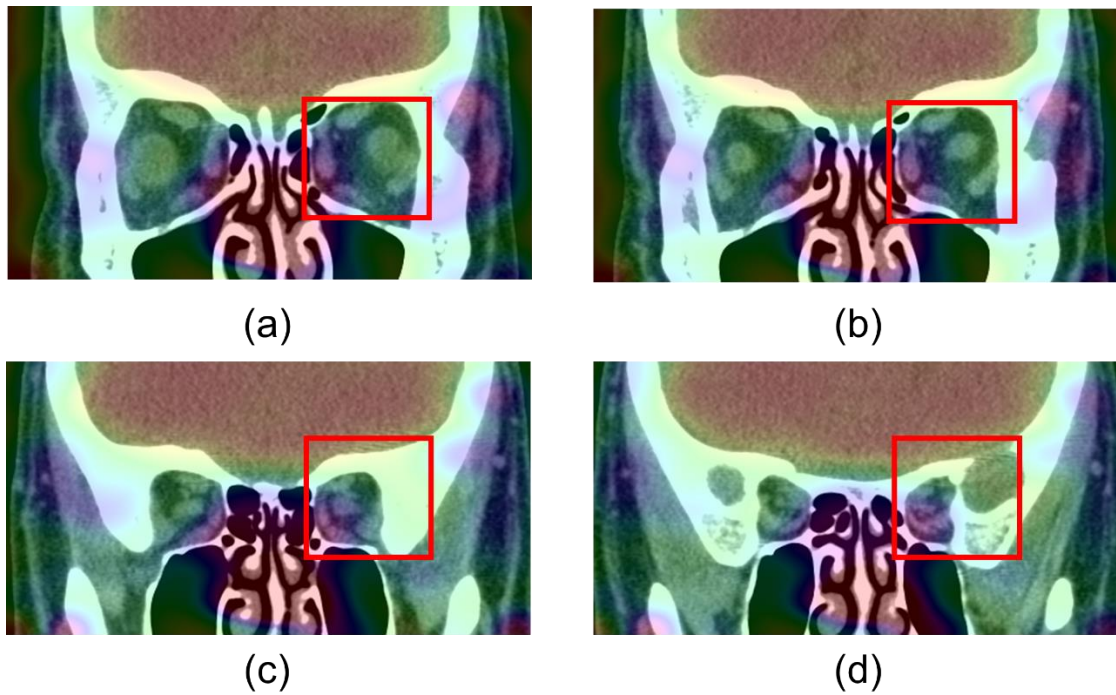
The first row is a slice of the GO patient's left eye, and the second row is a slice of the right eye of the GO patient. The red contours in all slices represent the ground truth. Colors in the annotations reflect the contours of segmentation results: blue, MR; purple, SR; yellow, LR; yellow, IR.

**Supplemental Fig. 3 Three-dimensional morphology and function of EOMs derived from orbital SPECT/CT.**



(a) 3D morphology of EOMs derived from CT (b) DTPA uptake of EOMs derived from SPECT.

**Supplemental Fig. 4 Coronal views of SPECT/CT fusion image.**



The red box marks the eye of interest, a patient who experienced high uptake of DTPA in the adjacent sinuses, leading to the misinterpretation of their medial rectus and inferior rectus muscles by the model as areas where lesions occurred. (a), (b), (c), (d): different slices of SPECT/CT fusion images.